

DualLQR: Efficient Grasping of Oscillating Apples using Task Parameterized Learning from Demonstration

Robert van de Ven¹, Ard Nieuwenhuizen², Eldert J. van Henten¹, and Gert Kootstra¹

Abstract—Learning from Demonstration offers great potential for robots to learn to perform agricultural tasks, specifically selective harvesting. One of the challenges is that the target fruit can be oscillating while approaching. Grasping oscillating targets has two requirements: 1) close tracking of the target during the final approach for damage-free grasping, and 2) the complete path should be as short as possible for improved efficiency. We propose a new method called DualLQR. In this method, we use a finite horizon Linear Quadratic Regulator (LQR) on a moving target, without the need of refitting the LQR. To make this possible, we use a dual LQR setup, with an LQR running in two separate reference frames. Through extensive simulation testing, it was found that the state-of-art method barely meets the required final accuracy without oscillations and drops below the required accuracy with an oscillating target. DualLQR was found to be able to meet the required final accuracy even with high oscillations, with an accuracy increase of 60% for high orientation oscillations. Further testing on a real-world apple grasping task showed that DualLQR was able to successfully grasp oscillating apples, with a success rate of 99%.

I. INTRODUCTION

Learning from Demonstration (LfD) offers great potential for robots to learn to perform tasks through human demonstrations, removing the need for programming complex motions into robots, which is a time-expensive task in variable environments [1]. LfD has been implemented for various tasks, such as in-home assistance [2], in agricultural [3], [4], [5], and industrial tasks [6]. However, many domain-specific challenges remain unaddressed.

Within agricultural tasks, LfD is valuable for selective harvesting. Selective harvesting is challenging to automate because of variation and specific detachment motions required for safe harvesting of different types of fruits [7]. In selective harvesting, manipulators are used in three phases: 1) approach to target fruit, 2) detachment of fruit from the plant, and 3) placement of fruit in a storage container [8]. In the approach phase, the manipulator must approach the fruit safely, without damaging the plant or the fruit. One of the challenges during the approach phase is a moving target fruit [9]. This moving can occur because of hitting a compliant branch during the harvest operation, because of removing other fruits from the same branch or because of

wind. Due to the compliance in a branch, this can result in long-lasting oscillations of the fruit. To still be able to grasp the fruit, the robot needs to adapt to the oscillation. To deal with the oscillation of a target, visual servo control has been used, but has trouble dealing with occlusions and cases of large movement due to collisions between the end-effector and the fruit [10]. This challenge of oscillating targets has not yet been addressed and solved in harvesting robotics [9], let alone for LfD in selective harvesting.

In LfD, tracking moving targets has been studied before. Research has focused on grasping moving objects from conveyors [6], [11], catching or hitting flying objects [12], [13], or grasping a moving target during the task execution [14], [15], [16]. However, these studies did not focus on tracking the target only when close to grasping and the target's movement was not oscillatory. For selective harvesting, oscillations are the most common movements and tracking should only occur when close to the target, to reduce the length of the path and be able to speed up the task execution. Therefore, an LfD algorithm for selective harvesting has two requirements: 1) close tracking of the target during the final approach for damage-free grasping, and 2) the complete path should be as short as possible for improved efficiency. The combination of these two requirements adds a requirement for information on when tracking is important.

To combine these requirements, two reference frames should be used. The first frame will be placed at the pose of the target for close tracking during the final approach. The second frame will be placed at the initial pose of the end-effector for reduced tracking behaviour when further away. By transforming the demonstrations to each reference frame, the variation in the demonstrations in each reference frame can be used as information on when tracking is important. Task Parameterized Gaussian Mixture Models (TP-GMM) combine these requirements [16]. Task Parameterization (TP) allows a task to be learned using multiple reference frames, transforming the demonstrations to each reference frame. In each reference frame, a GMM can be used to learn the variability of the demonstrations. By using multiple Gaussians, the variability can be learned in higher detail, e.g. variation over time and space. To transform the TP-GMM to trajectories that can be used by a robot, a regression method needs to be used, e.g. Gaussian Mixture Regression (GMR) and/or Linear Quadratic Regulator (LQR) [17].

Calinon et al. [16] proposed a TP-GMM and GMR, coupled to an infinite horizon LQR (InfLQR) to be able to deal with targets moving during execution. At each timestep, the method performs three steps: 1) combine the GMMs in

*This research is part of the research program SYNERGIA (project number 17626), which is partly financed by the Dutch Research Council (NWO).

¹Agricultural Biosystems Engineering, Wageningen University and Research, 6708PB Wageningen, The Netherlands. robert.vandeven@wur.nl

²Agrosystems Research, Wageningen University & Research, 6708 PB Wageningen, the Netherlands.

each reference frame given the new poses of the reference frames, 2) perform GMR on the combined GMM to extract the end-effector goal and covariance matrix, and 3) calculate control commands based on the output of the GMR using the InfLQR. By using an InfLQR, the method can calculate control commands without calculating the remaining trajectory at each timestep. The authors showed that the algorithm could execute the task with a moving target. However, no analysis of the performance was performed. InfLQR was used to limit computation time. This was important since the moving target would result in changes in the combined GMM, which would mean that a finite horizon LQR would need to be refitted on the complete remaining part of the trajectory. However, a finite horizon LQR is preferred since it can consider the varying precision in the remaining part of the task [16].

We propose a new method called DualLQR. In this method, we use a finite horizon LQR on a moving target, without the need of refitting the LQR, thereby reducing the computations in the real time loop. To make this possible, we use a dual LQR set-up, with an LQR running in two reference frames. On the GMM in each reference frame, GMR is performed to extract the mean and covariance matrix at each timestep. The LQR in that reference frame is then fitted to these means and covariance matrices. Since this is done in the reference frame, a moving target would only result in a changing current state from the view of the LQR. During execution, each LQR is used to calculate the desired control in that reference frame. These controls are combined using a weighted average based on the precision matrix of the GMR in that reference frame. For the apple harvesting task, one reference frame is the stationary initial pose of the end-effector and the other reference frame is the oscillating fruit. The effect of tight tracking during the final approach is achieved in two ways. First, each LQR will track tighter if the covariance is smaller, which will happen when the target pose is closer to the origin of the reference frame. Second, this effect is enhanced by using the weighted average of precision matrices. Therefore, the LQR in the reference frame with higher required precision will affect the combined control output more.

To evaluate the proposed method, we performed comprehensive simulation experiments testing the proposed method DualLQR and the existing method InfLQR [16] and comparing their performance. In addition, we tested the proposed method on a real robot on a simplified apple grasping task. Our code is available <https://github.com/WUR-ABE/DualLQR>.

II. PROPOSED METHOD

The proposed method has a demonstration phase, a learning phase, and a reproduction phase [18]. In the demonstration phase, a set of movements was recorded and processed to be used as data for the learning phase. The movements were recorded using the end-effector pose. In the learning phase, the TP-GMM was fitted to demonstrations in each reference frame using expectation-maximization (EM) [18].

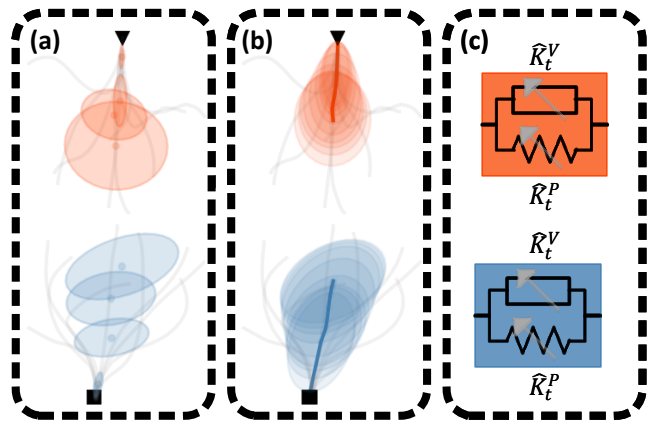


Fig. 1. Steps before execution. In each step, light grey lines show the demonstrations. Each step was performed separately in the start and end frames. The start frame is indicated in blue and the end frame is indicated in orange. (a) shows each reference frame’s GMM, where dots indicate the means and ellipses the covariances of the Gaussian components. (b) shows each reference frame’s GMR, where the line indicates the mean of the path and ellipses show the covariance along the path. (c) shows each reference frame’s LQR. The \hat{K}_t^P and \hat{K}_t^V indicate the gains, which are tuned using the GMR and an additional control cost ρ .

In the reproduction phase, we made several changes before and during the execution of a trajectory. In Section II-A, the steps before execution are described. In Section II-B, the steps during execution are described.

A. Before execution

Fig. 1 shows the steps before execution. In Fig. 1, the black square corresponds to the start reference frame and the black triangle corresponds to the end reference frame. These poses were used to obtain the GMM in each reference frame, see Fig. 1a. Then, we performed a Gaussian Mixture Regression to extract the mean and covariance matrix at each timestep in each reference frame, shown in Fig. 1b. In our case, means and covariance matrices contained the end-effector pose. The number of timesteps were determined using the duration of the demonstrations and the desired frequency of the online control loop. Lastly, the LQR was fitted to the output of the GMR [17], shown in Fig. 1c. Here, the control cost of the LQR was set to optimize the behaviour [17]. A lower control cost results in tighter tracking of the target, but will also increase the distance travelled.

B. During execution

Fig. 2 shows the steps during execution. The start frame is shown in blue and the end frame, which can be oscillating, is shown in orange. The first step is to transform the task from the world frame, shown in Fig. 2a, to the two reference frames, shown in Fig. 2b. In each reference frame i , the end-effector pose $x_{i,t}$ was provided to the LQR, shown in Fig. 2c. Since the LQRs were fitted before execution, each immediately calculated the control output. The last step was to combine the control output of each LQR, shown in Fig. 2d. The control outputs were transformed back into the world frame and the weighted average is calculated using the covariance matrix $\Sigma_{i,t}$ from each GMR i . Since we aimed to prioritise the reference frame with the least variance, we

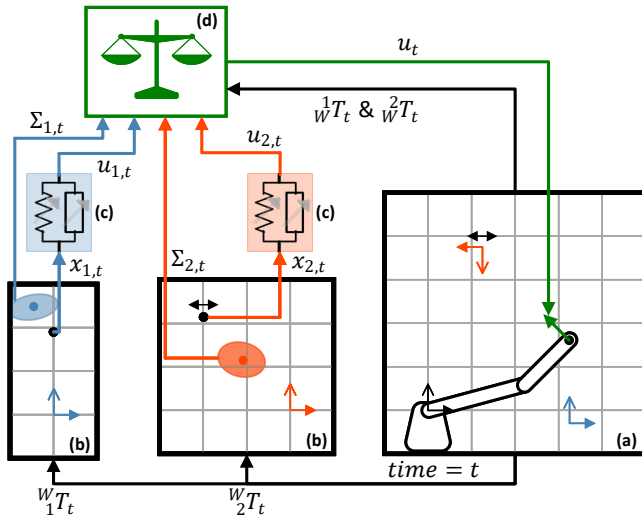


Fig. 2. Processes in the control loop during execution visualized in 2D. (a) indicates the task in the world frame, shown in black. The blue frame indicates the start frame and the orange frame indicates the end frame, which oscillates, as the black arrow indicates. The green vector is the control output provided by DualLQR. (b) indicates the task in each reference frame i , transformed using ${}^W_i T_t$ and with the covariance matrix $\Sigma_{i,t}$ from the GMR. Because of this transformation, the oscillation of the end-effector in the end-frame results in an oscillation of the end-effector in the end-frame. (c) indicates each LQR, using the end-effector pose $x_{i,t}$ as input. (d) indicates the balancing between the two LQRs, using $u_{i,t}$ and $\Sigma_{i,t}$, resulting in control output u_t .

used the inverse covariance matrix, i.e. the precision matrix. This resulted in the following equation:

$$u_t = \left(\text{diag}(\Sigma_{1,t}^{-1}) + \text{diag}(\Sigma_{2,t}^{-1}) \right)^{-1} \cdot \left(\text{diag}(\Sigma_{1,t}^{-1}) \cdot u_{1,t} + \text{diag}(\Sigma_{2,t}^{-1}) \cdot u_{2,t} \right) \quad (1)$$

With $u_{i,t}$ being the vector containing controls of LQR i at timestep t and $\Sigma_{i,t}$ being the covariance matrix of GMR i at timestep t . In our case, i can be 1 and 2, indicating the start and reference frames. Lastly, u_t is the vector containing the combined and weighted controls. The covariance matrix provided by the GMR is non-sparse. To ensure control output in one dimension does not influence control output in other dimensions, the covariance matrix is changed to a diagonal matrix by setting all non-diagonal values to zero.

From the combined controls and the current end-effector pose, the next end-effector pose was calculated. The last step was calculating the inverse kinematics to control the robot arm. This was done using the Levenberg-Marquardt Numerical Inverse Kinematics Solver.

III. EXPERIMENTS

We performed two experiments. First, we tested both InfLQR [16] and DualLQR in a simple simulation environment with different oscillations and controller settings. Next, we tested DualLQR in a real-world apple grasping task.

For both experiments, we used a model trained on 40 demonstrations. In these demonstrations, the target was a 10cm cube, which was static. Using a static target in the demonstrations simplified the process of collecting demonstrations. Fig. 3 shows the path of a typical demonstration,

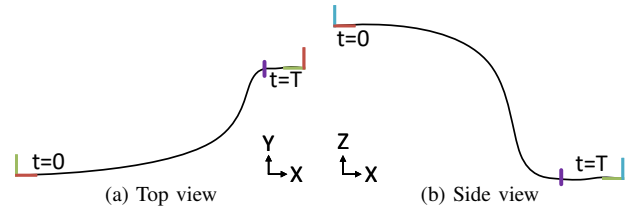


Fig. 3. Typical example of a demonstration. The wireframes indicate the start and end-frame. The purple line indicates the start of the final approach.

going from $t = 0$ to $t = T$. The same demonstration dataset was used as in Van de Ven et al. [19].

A. Simulation experiment

In the simulation experiment, we tested the infinite horizon LQR (InfLQR) [16] and our proposed DualLQR. The simulation was created using ROS2, using a simulated UR5e manipulator. The moving target was created by defining a target pose with sinusoidal movement on one dimension. In this experiment, we adjusted the control cost, the axis along which the oscillation took place and the amplitude of the oscillation. The control cost allowed optimization between the closeness of tracking and the total distance travelled by the manipulator. Through using different axes and amplitudes, we investigated the robustness and which oscillations were the most challenging for the methods. The control cost was adjusted between -3.0 and 3.0 in steps of 0.3 . The oscillation was performed along x , y , z , roll, pitch, and yaw. For the results, we grouped these into position or orientation oscillations. The oscillation amplitude was set at four levels, specifically no oscillation, low oscillation of 0.05 m or 0.15 rad, medium oscillation of 0.10 m or 0.30 rad, and high oscillation of 0.15 m or 0.45 rad.

In each test, we performed eleven repetitions, placing the goal in a new pose each time. We used one central pose at $[0.22, 0.27, -0.26, 0.00, 0.00, 1.46]$. The remaining ten poses changed one dimension, using the following values: X: ± 0.1 , Y: ± 0.2 , Z: ± 0.05 , roll: ± 0.2 , yaw: ± 0.2 . These poses were based on the variation in the demonstration dataset, which had minimal variation along the pitch axis.

The task of apple harvesting requires high accuracy in the final approach, combined with a short path. To calculate the accuracy in the final approach, the first step was to define the final approach. The start of the final approach is indicated in Fig. 3 using a purple line. In the end-frame, this point lies at $Y=0.05$ m. This point was chosen as it indicates the position from where collisions with the target can occur, which would result in failed grasps. As all demonstrations were successful, we used the median absolute deviations from the origin as the limits for the final approach phase. Staying below these limits indicates a successful final approach phase in the trajectory of an execution. These limits were 0.03 m along the Y-axis, 0.10 m along the Z-axis, 0.07 rad along the roll axis, 0.07 rad along the pitch axis, and 0.07 along the yaw axis. For each execution, we determined at what timestep the final approach started. From there, we calculated the fraction of timesteps where the end-effector pose was within these limits. We used

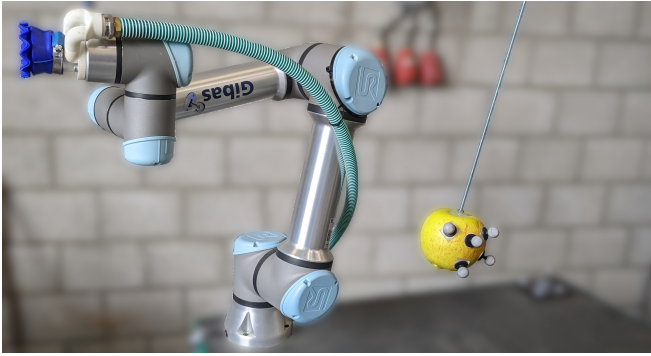


Fig. 4. Initial state of the apple grasping set-up

the fraction in the demonstrations, which was at 0.88, as the required accuracy. For the requirement of a short path, we looked at the distance the manipulator travelled to perform the task. This was calculated using the Euclidean distance in meters and the quaternion distance. These were calculated for all timesteps. This results in the following equation:

$$d = \sum_{t=1}^T (|p_t - p_{t+1}| + \min(|q_t - q_{t+1}|, |q_t + q_{t+1}|)) \quad (2)$$

With p being the position vector and q being the orientation, represented as quaternion.

Based on this analysis, we compared the optimal settings of both methods on key elements of the task. We compared the methods on final approach accuracy, Euclidean and rotation distance as included in Equation 2.

B. Apple grasping experiment

Next, we tested the performance of the method in a real-world environment while doing a harvesting task, specifically apple grasping using a suction cup gripper. Fig. 4 shows the initial state of the apple grasping set-up. On the left, the UR5e manipulator is shown. The end-effector is a suction cup. On the right, the apple is shown. We used a fake apple for the experiments, with OptiTrack [20] markers to track its pose. The apple was attached to a rod, oscillating in a pendulum motion, along the X-axis of the end-frame. Before each run, the apple was positioned at one of the extremes of the pendulum motion. At the start of each run, the apple was released, resulting in a dampened oscillating motion. Compared to the simulation experiment, the oscillation of the apple corresponds to the combination of a medium position oscillation and a medium orientation oscillation.

The goal of this experiment was to grasp the apple successfully. In addition to the aforementioned metrics of final accuracy and distance travelled, we evaluated the time until successful grasping. A successful grasp happened when the air pressure in the suction cup dropped below 0.9 bar. If this happened before the trajectory was completed, the time the pressure dropped below 0.9 bar was used as the time until successful grasping. Otherwise, the complete time to execute the trajectory was stored.

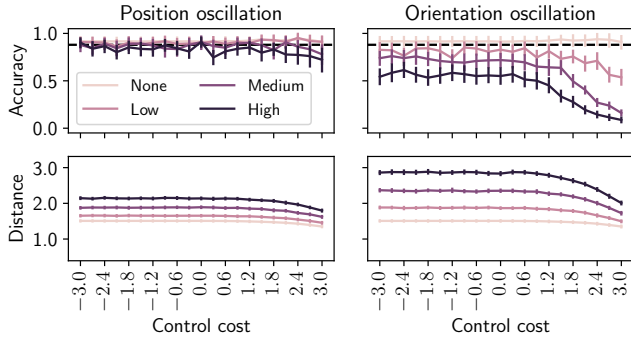
IV. RESULTS

A. Results simulation experiment

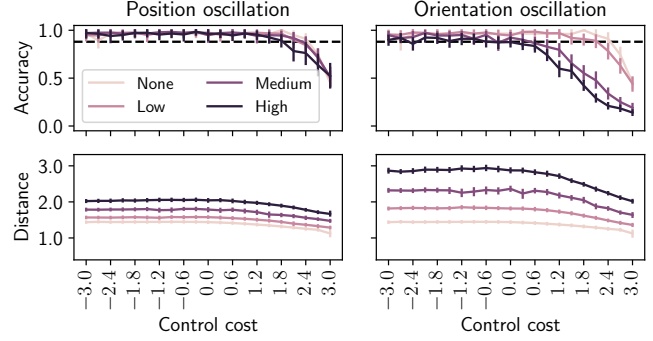
Fig. 5a shows the performance of InfLQR in terms of accuracy and distance travelled as a function of the control cost used. With increasing position oscillations, the accuracy dropped slightly. With high oscillations, only two controller settings reached the required accuracy, specifically at a control cost of 0.0 and -3.0 . A slight effect of control cost was observed, with higher control costs resulting in lower accuracy. The InfLQR was unable to correctly deal with orientation oscillations. From low oscillations, the method was unable to reach the required accuracy for any control cost. In addition, higher control costs reduced the accuracy. Each level of oscillation added more distance travelled by the manipulator. This effect was bigger for orientation oscillations, and reduced by increasing the control cost.

Fig. 5b shows the performance of the DualLQR in terms of accuracy and distance travelled as a function of the control cost used. The effect of the oscillations on the accuracy was much smaller compared to the InfLQR. Without oscillations, it can be seen that high control costs resulted in lower accuracy. To reach the required accuracy, the control cost needed to be 2.4 or lower. Introducing oscillations along the position of the target had a minimal effect on the accuracy. The value of control cost from which the required accuracy was reached dropped slightly. For low and medium oscillations, this was 2.1 or lower. For high oscillations, this was 1.8 or lower. Introducing oscillations along the orientation of the target resulted in a similar behaviour, but the accuracy of low control costs also dropped slightly. For low oscillations, the requirement was met at a control cost of 2.1 or lower. For medium oscillations, the controller reached the requirement from a control cost of 0.3 or lower, except for -0.3 . For high oscillations, the controller reached the requirement from a control cost of 0.0 or lower, except for -0.3 . Each level of oscillation added more distance travelled by the manipulator. This effect was bigger for orientation oscillations, and reduced by increasing the control cost.

To compare the methods, we selected the highest control cost that reached the required accuracy. For the InfLQR, we selected a control cost of 0.0, which was the highest control cost that reached the required accuracy under high position oscillations. For the DualLQR, we selected a control cost of 0.0 as well, this was the highest control cost that reached the required accuracy under high orientation oscillations. Table I shows the performance of both methods for all oscillations. DualLQR resulted in higher accuracy for all oscillations, increasing on average 18%. Only medium and high position oscillations did not result in significantly higher accuracy. For the Euclidean distance, similar results were observed, with an average decrease of 3.7%. For rotated distance, the DualLQR decreased the distance with an average of 2.8%. DualLQR performed better for position oscillations, while the InfLQR was better for high oscillations along the orientation. However, the much lower accuracy indicates worse tracking, which reduced the distance.



(a) Results of the simulation testing of the InfLQR.



(b) Results of the simulation testing of the Dual LQR.

Fig. 5. Results of the simulation testing of both methods. Darker lines indicate higher oscillation levels. The levels are described in section III-A. The figures on the left show the effect of an oscillation of the target’s position and the figures on the right show the effect of an oscillation of the target’s orientation. At each tested setting, a vertical bar indicates the 95% confidence interval. The black dashed line indicates the required accuracy, set at 0.88.

TABLE I

PERFORMANCE IN SIMULATION OF BEST MODELS FOR EACH OSCILLATION LEVEL & METHOD. BOLD VALUES INDICATE THE BEST METHOD WHEN THERE IS A SIGNIFICANT DIFFERENCE BETWEEN BOTH METHODS AT A P-VALUE OF 0.05.

Oscillation	Method	Accuracy	Translation	Rotation
None	DualLQR	0.96±0.11	0.59±0.039	0.85±0.036
	InfLQR	0.91±0.15	0.62±0.033	0.89±0.038
Low, Ori	DualLQR	0.95±0.16	0.61±0.041	1.21±0.060
	InfLQR	0.83±0.23	0.63±0.033	1.24±0.057
Low, Pos	DualLQR	0.98±0.10	0.73±0.043	0.84±0.036
	InfLQR	0.90±0.15	0.76±0.039	0.89±0.038
Medium, Ori	DualLQR	0.92±0.15	0.66±0.081	1.71±0.131
	InfLQR	0.72±0.20	0.66±0.039	1.69±0.096
Medium, Pos	DualLQR	0.95±0.16	0.94±0.102	0.85±0.045
	InfLQR	0.91±0.19	1.00±0.046	0.89±0.040
High, Ori	DualLQR	0.88±0.13	0.65±0.044	2.22±0.140
	InfLQR	0.55±0.25	0.69±0.053	2.14±0.135
High, Pos	DualLQR	0.96±0.14	1.20±0.078	0.84±0.047
	InfLQR	0.91±0.14	1.23±0.054	0.91±0.039

B. Results apple grasping experiment

When testing the performance of DualLQR on apple grasping, we found a very high success rate. Only a single grasp attempt out of 110 was unsuccessful, at a control cost of -0.3 , shown with a cross in Fig. 6. For this control cost, the final approach accuracy was also insufficient, as shown in Fig. 6. From -0.9 , the required accuracy was met, except for -2.1 . At this control cost, the apple yaw of the apple was around 0.3 less than the other settings.

In this experiment, the control cost needed to be lower to achieve the required accuracy, as shown in the top plot in Fig. 6. However, similar accuracy was achieved with low control costs. Furthermore, the distance travelled by the manipulator was nearly doubled compared to the simulation, as shown in the middle plot in Fig. 6. Lastly, the bottom plot of Fig. 6 shows that the time until successful grasping was the lowest at a control cost of -1.2 . At a control cost of -1.8 or lower, there was a lot of variation, while control costs above -1.2 were slightly slower.

Both effects were caused by the interaction between the

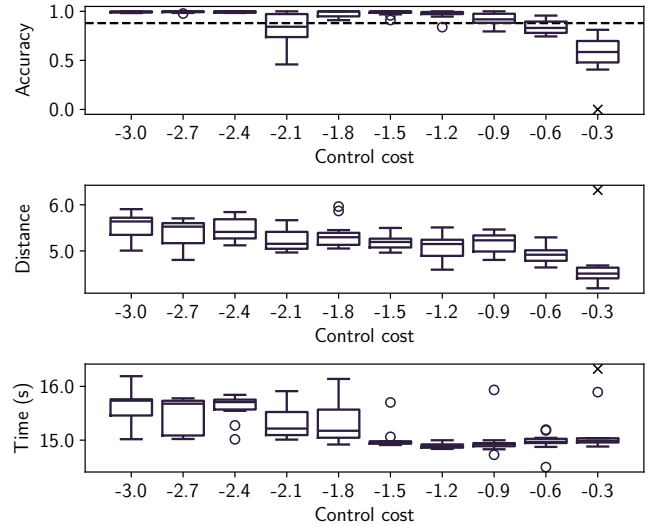
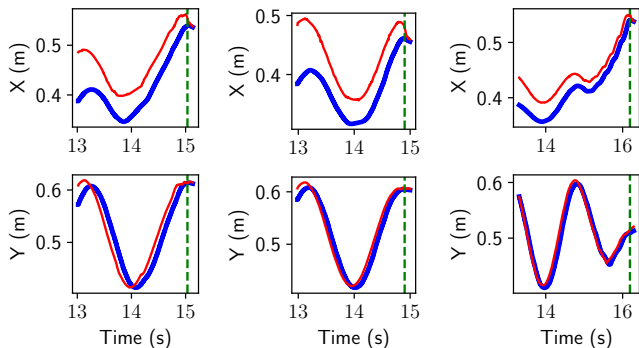


Fig. 6. Boxplots of results of testing the Dual LQR on apple grasping. X indicates a failed attempt.

suction cup and apple, shown in Fig. 7. Fig. 7a shows the behaviour at a control cost of -0.3 . In this case, the apple was not tracked close enough for successful grasping. Instead, the side of the suction cup collided with the apple. This contact between the apple and the suction cup occurred close to the grasping. In the contact, the apple slipped over the suction cup, reducing speed and rotating slightly, which occurred just after 14 seconds, where the red line has sudden changes in the Y and X plot. Fig. 7c shows the behaviour at a control cost of -3.0 . In this case, the apple was tracked accurately. If the apple was not immediately grasped at first contact, the manipulator would push the apple away and react quickly, pushing it further away. This contact between the apple and the suction cup occurred multiple times close to the grasping. In this contact, the apple bounced off the flexible suction cup until the contact was good enough to create a vacuum. This can be seen in Fig. 7c, where there are multiple sudden changes in the X plot, as the fruit is moved further away. Fig. 7b shows the behaviour at a control cost of -1.2 . With control cost -1.2 , these two effects were balanced optimally, resulting in the fastest grasping. No perceivable contact occurred between the apple and the suction cup until



(a) Control cost of -0.3 (b) Control cost of -1.2 (c) Control cost of -3.0

Fig. 7. Trajectory of final approach along X and Y. The red line indicates the pose of the target and the blue line indicates the pose of the robot. The green vertical line indicates the time of successful grasping.

the grasp. This can be seen in the smooth trajectory of the target in Fig. 7b.

V. DISCUSSION

DualLQR increased the final approach accuracy by 60% and reduced the distance travelled compared to the InfLQR. This was due to the use of the finite horizon LQR and reducing the computations in the real time loop, allowing for faster responses to changes in the target pose. In addition, the difference in required precision between the reference frames was used twice. First in the fitting of each LQR, where higher precision resulted in larger control outputs. Next, it was used again when combining the outputs. This increased the effect.

In order to evaluate the performance of the methods, we used the final approach accuracy as a metric. Related work primarily used the accuracy at the final pose [21], [3]. However, this does not take the approach into account, where collisions can result in additional movement of a target or damage to a target. However, the final-approach-accuracy metric also leaves room for improvement. In the apple grasping experiment, the DualLQR was able to grasp apples successfully despite not meeting the required accuracy. The metric can be adjusted to calculate deviation from a desired path. However, a desired path would need to be defined.

In the apple grasping experiment, the OptiTrack system and using a real manipulator added roughly 45 ms of latency to the control loop between a movement of the target in the world and an action of the manipulator. Combined with the dynamics required to move the manipulator, this resulted in a reduced accuracy compared to the simulation experiment. Using a camera and processing to obtain the pose of the fruit will add even more time. One of the ways this latency can be addressed is by using a predictor to estimate the future pose of the fruit, e.g. by using Model Predictive Control [22]. This can improve the performance of the proposed method in the apple grasping experiment, where the apple was oscillating consistently. However, in the case of a real apple tree, this prediction will be more challenging, due to variable flexibility in branches, wind, and other operations in the same tree. In our experiments, we found that lower control costs result in similar performance between the simulation and real

environment. In a system with increased latency, even lower control costs might be required.

Through the OptiTrack system, we obtained a continuous and precise pose of the apple. In a real scenario, a vision system will be less reliable. When far away, the influence of incorrect pose estimation will be minimized. As the robot approaches the fruit, the pose estimation is expected to improve, and DualLQR can adjust for these improvements. However, when very close to the fruit, the robot can block the view of the fruit. Therefore, further sensorization of the system might be needed to obtain the pose of the apple when very close to the fruit.

In the apple grasping experiment, a reduced accuracy did not yet lead to reduced grasping success. The suction cup was continuously sucking and showed a tolerance for misalignment of around 1cm. If the apple was within the tolerance at some point during the action, the apple would be grasped. This effect increased the success rate. However, contact also occurred with greater misalignment, which caused the apple to bounce off. At low control costs, repeated bouncing could occur due to the fast movement of the manipulator after the initial bounce. While the contact itself is not expected to cause damage to real apples due to the use of soft silicon, the movement caused by the interaction could cause damage to the branch or peduncle. In addition, higher accuracy would be required if an encompassing gripper was used.

For the DualLQR, we used two reference frames. The methods can be extended to include any number of reference frames. This can then be extended to e.g. obstacle avoidance, if an algorithm provides the importance of the obstacle avoidance through a covariance matrix.

VI. CONCLUSION

In this work, we presented DualLQR, a novel Learning from Demonstration method aimed at approaching oscillating targets while only tracking the oscillation near the target. Through extensive simulation testing, it was found that InfLQR barely meets the required final accuracy without oscillations and drops below the required accuracy with an oscillating target. DualLQR was found to be able to meet the required final accuracy even with high oscillations. Both methods performed best at a control cost of 0.0. Comparing these settings, DualLQR increased the accuracy 18% compared to InfLQR, with the largest improvement being an increase of 60% with high orientation oscillations. In addition, the translated and rotated distances were reduced by 3.7% and 2.8% respectively.

Further testing in a simplified apple grasping experiment showed that DualLQR can successfully grasp oscillating apples, with a success rate of 99%. The optimal control cost was found to be -1.2 . Here, grasping the apple was done in 14.9 seconds on average, compared to 15.6 seconds for the slowest control cost setting. In addition, the fruit was not touched before grasping. Higher control costs reduced the distance travelled, but also increased the time to grasp.

REFERENCES

- [1] A. G. Billard, S. Calinon, and R. Dillmann, *Learning from Humans*. Cham: Springer International Publishing, 2016, pp. 1995–2014. [Online]. Available: https://doi.org/10.1007/978-3-319-32552-1_74
- [2] N. Figueroa and A. Billard, “Locally active globally stable dynamical systems: Theory, learning, and experiments,” *The International Journal of Robotics Research*, p. 02783649211030952, 2022.
- [3] A. Tafuro, B. Debnath, A. M. Zanchettin, and E. A. Ghalamzan, “dpmp-deep probabilistic motion planning: A use case in strawberry picking robot,” in *2022 IEEE/RSJ International Conference on Intelligent Robots and Systems (IROS)*. IEEE, 2022, Conference Proceedings, pp. 8675–8681.
- [4] K. Motokura, M. Takahashi, M. Ewerton, and J. Peters, “Plucking motions for tea harvesting robots using probabilistic movement primitives,” *IEEE Robotics and Automation Letters*, vol. 5, no. 2, pp. 3275–3282, 2020.
- [5] P. La Hera, D. O. Morales, and O. Mendoza-Trejo, “A study case of dynamic motion primitives as a motion planning method to automate the work of forestry cranes,” *Computers and Electronics in Agriculture*, vol. 183, p. 106037, 2021.
- [6] K. Yamamoto, H. Ito, H. Ichiwara, H. Mori, and T. Ogata, “Real-time motion generation and data augmentation for grasping moving objects with dynamic speed and position changes,” *arXiv preprint arXiv:2309.12547*, 2023.
- [7] G. Kootstra, X. Wang, P. M. Blok, J. Hemming, and E. Van Henten, “Selective harvesting robotics: current research, trends, and future directions,” *Current Robotics Reports*, vol. 2, no. 1, pp. 95–104, 2021.
- [8] J. Davidson, S. Bhusal, C. Mo, M. Karkee, and Q. Zhang, “Robotic manipulation for specialty crop harvesting: A review of manipulator and end-effector technologies,” *Global Journal of Agricultural and Allied Sciences*, vol. 2, no. 1, pp. 25–41, 2020.
- [9] W. Au, H. Zhou, T. Liu, E. Kok, X. Wang, M. Wang, and C. Chen, “The monash apple retrieving system: A review on system intelligence and apple harvesting performance,” *Computers and Electronics in Agriculture*, vol. 213, p. 108164, 2023.
- [10] V. Rajendran, B. Debnath, S. Mghames, W. Mandil, S. Parsa, S. Parsons, and A. Ghalamzan-E, “Towards autonomous selective harvesting: A review of robot perception, robot design, motion planning and control,” *Journal of Field Robotics*, 2023.
- [11] R. Prakash, L. Behera, S. Mohan, and S. Jagannathan, “Dual-loop optimal control of a robot manipulator and its application in warehouse automation,” *IEEE Transactions on Automation Science and Engineering*, vol. 19, no. 1, pp. 262–279, 2020.
- [12] S. Kim, A. Shukla, and A. Billard, “Catching objects in flight,” *IEEE Transactions on Robotics*, vol. 30, no. 5, pp. 1049–1065, 2014.
- [13] R. Prakash, L. Behera, S. Mohan, and S. Jagannathan, “Dynamic trajectory generation and a robust controller to intercept a moving ball in a game setting,” *IEEE Transactions on Control Systems Technology*, vol. 28, no. 4, pp. 1418–1432, 2019.
- [14] R. Pérez-Dattari and J. Kober, “Stable motion primitives via imitation and contrastive learning,” *arXiv preprint arXiv:2302.10017*, 2023.
- [15] L. Wang, Q. Li, J. Lam, Z. Wang, and Z. Zhang, “Intent inference in shared-control teleoperation system in consideration of user behavior,” *Complex & Intelligent Systems*, pp. 1–11, 2021.
- [16] S. Calinon, D. Bruno, and D. G. Caldwell, “A task-parameterized probabilistic model with minimal intervention control,” in *2014 IEEE International Conference on Robotics and Automation (ICRA)*. IEEE, 2014, Conference Proceedings, pp. 3339–3344.
- [17] S. Calinon and D. Lee, *Learning Control*. Dordrecht: Springer Netherlands, 2019, pp. 1261–1312. [Online]. Available: https://doi.org/10.1007/978-94-007-6046-2_68
- [18] S. Calinon, “A tutorial on task-parameterized movement learning and retrieval,” *Intelligent Service Robotics*, vol. 9, no. 1, pp. 1–29, 2016.
- [19] R. van de Ven, A. L. Shoushtari, A. Nieuwenhuizen, G. Kootstra, and E. J. van Henten, “Using learning from demonstration (lfd) to perform the complete apple harvesting task,” *Computers and Electronics in Agriculture*, vol. 224, p. 109195, 2024.
- [20] J. S. Furtado, H. H. T. Liu, G. Lai, H. Lacheray, and J. Desouza-Coelho, “Comparative analysis of optitrack motion capture systems,” in *Canadian Society for Mechanical Engineering International Congress 2018*, ser. Advances in Motion Sensing and Control for Robotic Applications. Springer International Publishing, 2019, Conference Proceedings, pp. 15–31.
- [21] C. Lauretti, C. Tamantini, H. Tomè, and L. Zollo, “Robot learning by demonstration with dynamic parameterization of the orientation: An application to agricultural activities,” *Robotics*, vol. 12, no. 6, p. 166, 2023.
- [22] K. Holkar and L. M. Waghmare, “An overview of model predictive control,” *International Journal of control and automation*, vol. 3, no. 4, pp. 47–63, 2010.